MEASUREMENT OF VOID FRACTION AND PARTICLE VELOCITY IN GAS-POWDER STREAMS BY CAPACITANCE TRANSDUCERS

G.A. Irons* and J.-S. Chang**,
* Department of Metallurgy and Materials Science and ** Department of Engineering Physics, McMaster University, 1280 Main Street West, Hamilton, Ontario, Canada L8S 4L7

ABSTRACT

A simple, economical and accurate technique, based on the different dielectric constants of solids and gases, has been developed to determine instantaneous, in situ void fractions and particle velocities in gas-powder streams. Two different electrode configurations were investigated for sensitivity and flow-regime dependency. Static, as well as high speed cinematographic, calibrations were performed. The technique is suitable for process control.

1. INTRODUCTION

Many plasma devices rely on very specific powder feeding conditions for their efficiency; however, particle velocities and void fraction are often poorly known. The object of the present work was to develop a simple technique to measure the instantaneous, volume-average in situ void fraction and particle velocity.

Of all the void fraction, or particle fraction measurement techniques available[1], the conductance probe and γ-densitometer methods seem to have been the most widely used. However, the conductance probe method has the disadvantage of being applicable only to electrically conductive particles and is signficantly influenced by a space charge in the environment. The disadvantages of γ-densitometery are that it exhibits a strong flow-regime dependence and requires a relatively strong source and thus, a large amount of radiation shielding, to observe fast transient phenomena.

The methods that have perhaps received the least amount of attention are capacitance probe techniques[2-3] and fast or thermal neutron scattering methods[4-5]. The fast or thermal neutron scattering methods also have shielding problems and the thermal neutron technique is particularly flow-regime dependent. The capacitance probe method has the following advantages: (i) most economical, (ii) simple installation, (iii) the electrodes are external to the flow, (iv) applicable to fast transient phenomena (up to a few μsec), and (v) the output is an analog voltage suitable for process control.

While such capacitance techniques have been investigated for diagnostics in packed and fluidized beds[2] and gas-liquid systems[3], the effects of electrode geometry and flow-regime dependence are unknown for flow in pipes. The development of such a technique and the assessment of such problems are the subjects of this paper.

When particles having a dielectric constant, K_2, are inserted between two electrodes separated by a gas having a dielectric constant, K_1, one will measure an effective dielectric constant, K_{EFF}, which will depend on K_1, K_2, the proportion and size of the particles, the electrode spacing, and the particle shape and distribution. Theoretical analysis for evenly distributed particles has delineated two possible limits of behaviour: the so-called parallel and series limits[2]. These are shown in Figure 3 and correspond to the cases of the two materials acting as two capacitors in parallel and series. Other workers have proposed different behaviour between these two limits[2]. The present approach has been more practical in that the effective capacitance was measured as a function of the above-mentioned variables.

Although no experiments were conducted, theoretical analyses do point to the applicability of such a transducer in a ionized, charged particle environment.

2. EXPERIMENTAL APPARATUS AND PROCEDURE

2.1 Stationary Experiments

Two basic electrode configurations designated, "ring" and "strip", as shown in Figure 1, were evaluated in these tests for sensitivity and flow-regime dependency. The glass tube was 210 mm long by 25 mm i.d. The ring electrodes consisted of two 9 mm wide aluminum strips attached circumferentially to the tube and separated by 11 mm. The strip electrodes consisted of two 35 mm long by 9 mm wide strips attached longitudinally and separated by 1.5 mm. (A limited amount of experimentation with various configurations determined these dimensions).

The void fraction was controlled by inserting known amounts of powder or a lucite test section in the tube. The shape of the lucite tube (Figure 5) simulated stratified, core, and annular flow of powder.

2.2 Dynamic Experiments

The most sensitive electrode configuration consisted of two brass plates 20 x 90 mm^2 wrapped around the glass tube (12.6 mm i.d., 19.0 mm o.d.) through which the powder flowed, as shown in Figure 2. This was wrapped with 5 mm of rubber and then electrostatically shielded with aluminum foil.

To determine K_{EFF} and hence, θ, one must identify the effect of the capacitance of the glass tube and leads. This was done by filling the tube with liquids having known dielectric constants. The results demonstrated that the material in the tube (having K_{EFF}) acted essentially as a series capacitor with the glass and leads.

Therefore, in actual powder tests, one could determine the capacitance of the leads and glass and the capacitance of the empty tube by measuring the capacitance with the tube empty and full of powder of a known packing density. This was done for the sand particles having a packing density of 58% (measured independently) and a dielectric constant of 4.0[6]. It was assumed that the gas and particles acted in series. This fixed the uppermost point in Figure 3.

Since the particle fraction, θ, for dispersed flow is much smaller than in the packed stated, separate calibration was undertaken. This was done by simultaneously measuring the capacitance, the particle mass flow rate (by weighing the discharge), and particle velocity, U_p, (by high speed

cinematography). The solids fraction is: $\theta = U_{ps}/U_p$ where U_{ps} is the superficial particle velocity. The results in Figure 3 show that a good working relationship between K_{EFF} and θ was obtained over a wide range of θ. (Note: this analysis does not prove the equivalent circuit is series.)

For the quantitative results reported in Figures 7 and 8, the random experimental error was mainly due to drift and fluctuations in the readings. A reasonable value for the error is considered to be one-half of the worst possible error (i.e., the average reading plus two standard deviations combined with the empty readings minus two standard deviations) which was on average 8% of the θ value, and is analogous to one standard deviation.

3. EXPERIMENTAL RESULTS AND DISCUSSION

3.1 Stationary Experiments

The relationship between measured output capacitance of the ring electrodes and void fraction in stratified systems are shown in Figure 4 for 40 μm diameter iron, 44 and 450 μm diameter silica powders. Figure 4 shows that the output capacitance is only linearly dependent on the void fraction when θ/θ_F is smaller than approximately 0.5 (θ_F is the particle fraction for a packed bed). Figure 4 also shows that conductive particles such as iron can be measured with the present technique.

The flow-regime dependence of the output capacitance is shown in Figure 5 for ring and strip electrodes. By comparison, one can see that the ring electrode geometry is less influenced by the flow-regime than the strip geometry. However, the ratio of the capacitance of a full tube to an empty one is much larger in the case of the strip electrode geometry than the ring electrode geometry. From this, one can conclude that the strip electrodes are more sensitive and are most useful when the flow-regime is known, whereas the ring electrodes are most useful when the flow-regime is unknown or rapidly changing.

3.2 Dynamic Experiments

The capacitance transducers can be used in the characterization of flow regimes, both steady and unsteady state. Figure 6b shows the capacitance output for the various flow regimes in Figure 6a for upward-flowing powder. The regime was determined by visual observation. The powder flow rate was increased in steps and the solids fraction, θ, can be seen to increase as well. With this particular apparatus, the flow became unsteady at $\theta = 0.03$, as seen by the variations in the output and visually by a "wavy" or "ropy" pattern. With further increases in solids loading, the particles could not be moved continuously and slugging of powder started. The slug loading and duration can be measured from Figure 6b.

This transducer is a very useful diagnostic tool in the dispersed regime, as shown in Figure 7, where the solids fraction, θ, was measured at various solid mass flow rate, W, and gas volumetric flow rate, Q, combinations at the lower transducer. If the particles and gas were travelling at the same speed (homogeneous flow), then θ would be given by

$$\theta_H = \frac{U_{ps}}{U_{gs} + U_{ps}} \qquad \text{(Eq. 1)}$$

shown by the dotted lines in Figure 7. Figure 7 shows that θ values are

generally higher than predicted by homogeneous flow. This is more clearly understood by transforming the variables to actual average gas and particle velocities.

$$U_p = \frac{U_{ps}}{\theta} = \frac{W}{A\rho\theta} \qquad \text{(Eq. 2)}$$

$$U_g = \frac{U_{gs}}{(1-\theta)} = \frac{Q}{A(1-\theta)} \qquad \text{(Eq. 3)}$$

where A is the cross-sectional area of the pipe and ρ is the density of the solid material.

From such a transformation, Figure 8, one can observe that these particles (average diameter - 450 μm, density - 2640 $kg \cdot m^{-3}$) have an appreciable slip velocity, which is in good accord with that which can be calculated from single particle correlations[7]. The high speed cinematography results also agree reasonably well. There is considerable divergence at higher velocities because the particles do not have sufficient time to accelerate to the fully developed flow case, although one can see that the particles passing a higher transducer are closer to the single particle slip line.

3.3 Application to Plasma Environments

To apply the present technique to flowing gas-powder-plasma streams, disturbances caused by ions and charged particles must be considered. If we assume quasi-steady state, the electric field is governed by Poisson's equation:

$$\nabla^2 V = -e(N_+ - N_- + N_{p+} - N_{p-})/\bar{\varepsilon} \qquad \text{(Eq. 4)}$$

where V is the electric potential, e is the electric charge, $\bar{\varepsilon}$ is the net permittivity of space, N is the number density, and the subscripts p, +, and - refer to charged particle, positive and negative ions, respectively. By introducing nondimensional parameters $\phi = eV/kT$, $\nabla = d\nabla$, $n = N/N_0$ and $\lambda_D = (\bar{\varepsilon}\, kT/e^2 N_0)^{1/2}$, the above equation becomes

$$\nabla^2 \phi = -(d/\lambda_D)^2 (n_+ - n_- + n_{p+} - n_{p-}) \qquad \text{(Eq. 5)}$$

where T is the ion temperature, k is Boltzmann's constant, d is the tube diameter, and N_0 is the normalized plasma density. For $d/\lambda_D < 1$, i.e., lower plasma density or higher temperature, the above equation reduces to Laplace's equation. Therefore, no significant field disturbance is expected. For smaller void fraction, most of the ions will be captured by particles and recombined in the surfaces[8]. Therefore, a small space charge effect is expected. For larger d/λ_D or void fraction, the present technique should be carefully applied.

4. CONCLUSIONS

A simple reliable capacitance technique has been developed to characterize gas-powder flow-regimes, as well as to determine void fraction and particle velocity.

REFERENCES

(1) G.F. Hewitt, "Measurement of Two-Phase Flow Parameters", (Academic Press, New York, 1978).
(2) T.B. Jones, General Electric Technical Information Series, Report No. 79 CRD 131, (Schenectady, NY, 1979).
(3) L. Cimorelli and R. Evangelisti, Int. J. Heat & Mass Transfer, 10, 277 (1967).
(4) R.A. Moss and A.J. Kelly, Int. J. Heat & Mass Transfer, 13, 491 (1970).
(5) C.N. Jackson, R.T. Alleman and W.G. Spear, Trans Am. Nucl. Soc., 11, 366 (1968).
(6) Handbook of Physics and Chemistry, edited by R.C. Weast, (CRC, Cleveland, 1971).
(7) R. Clift, J.R. Grace and M.E. Weber, "Bubbles, Drops and Particles", (Academic Press, New York, 1979).
(8) J.S. Chang, K. Kodera and T. Ogawa, Conference Record of 1978 IEEE Industry Application S.O.S., 38 (1978).

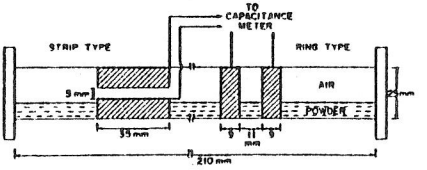

Figure 1: Schematic cross-sections of the strip and ring electrodes used in the stationary experiments.

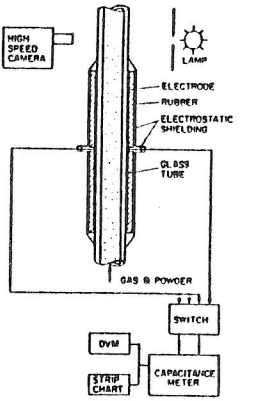

Figure 2: Schematic cross-section of the strip electrodes used in the dynamic experiments.

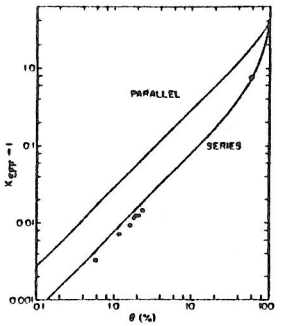

Figure 3: Calibration of strip electrodes for the dynamic experiments using high-speed cinematography. The theoretical parallel and series limits are also shown.

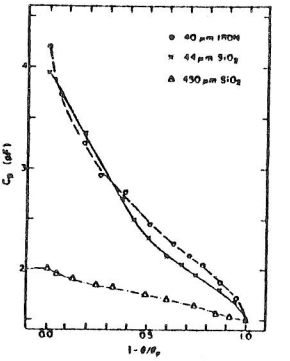

Figure 4: Output from the ring electrode as a function of θ in stationary, stratified configuration.

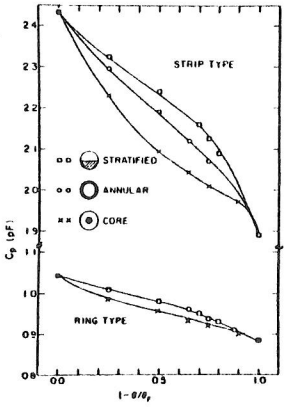

Figure 5: Output from strip and ring electrodes for stationary, lucite simulations of stratified, annular and core flow.

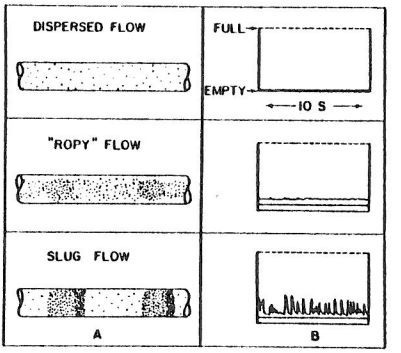

Figure 6(A): Visual appearance of upward, vertical flow in the pipe with increasing solids flow rate (top to bottom).

Figure 6(B): Traces from strip chart (output proportional to capacitance) for the various flow regimes.

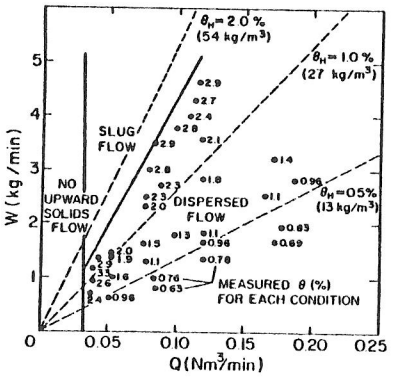

Figure 7: Measured θ in % at various solids, W, and gas, Q, flow rates. Solid lines delineate the regimes, the transition from dispersed to slug was judged when θ fluctuated significantly from the average. Dotted lines indicate various θ in homogeneous flow.

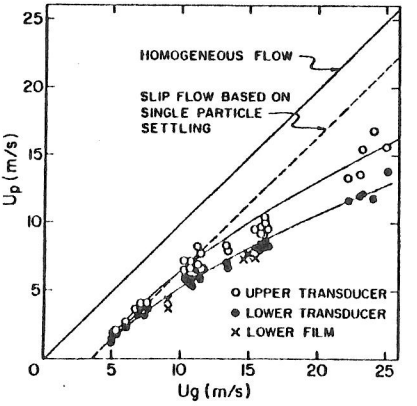

Figure 8: In-situ gas and particle flow rate from experiments in Figure 7. Upper and lower transducers were 0.6 m apart.